

Synthesis, Characterization, and X-ray Structural Analysis of Diplatinum Complexes Containing Bridging μ -SiHAr Ligands, $\{(\text{Ph}_n\text{Me}_{3-n}\text{P})_2\text{Pt}[\mu\text{-SiHAr}]\}_2$ [$n = 0-2$; Ar = 2-isopropyl-6-methyl(phenyl)]

J. Braddock-Wilking,^{*,†} Y. Levchinsky, and N. P. Rath

Department of Chemistry, University of Missouri—St. Louis, St. Louis, Missouri 63121

Received July 24, 2000

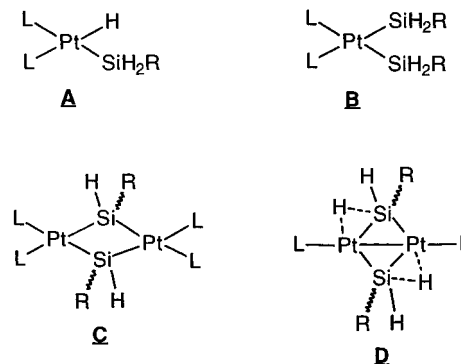
Reaction of (IMP)SiH₃ with (Ph_nMe_{3-n}P)₂PtMe₂ at 50 °C provided the dinuclear complexes *trans*-[(Ph_nMe_{3-n}P)₂Pt(μ-SiHAr)]₂ [Ar = 2-isopropyl-6-methylphenyl (IMP)]. These complexes were characterized by multinuclear NMR and IR spectroscopy and X-ray crystallography. The ²⁹Si NMR chemical shift for {(PhMe₂P)₂Pt[μ-SiH(IMP)]}₂ appears at unusually high field (−134 ppm) for complexes containing bridging silylene moieties. The X-ray structures of these complexes reveal acute Si–Pt–Si and obtuse Pt–Si–Pt angles. In solution, {(Ph₂MeP)₂Pt[μ-SiH(IMP)]}₂ undergoes dissociation of PMePh₂ down to −90 °C.

Introduction

The stoichiometric interaction of hydrosilanes with transition metal complexes can provide a diverse range of products depending upon the metal precursor used (Chart 1).¹ For example, sterically unhindered primary silanes (RSiH₃) react with Pt(0) precursors to produce dinuclear Pt₂Si₂ complexes with μ-SiHR groups bridging the platinum centers (C, Chart 1) or mononuclear bis(silyl) complexes (B, Chart 1).^{2–6} However, sterically demanding groups at silicon can provide mononuclear, P₂Pt(H)SiH₂R complexes (A, Chart 1). Secondary silanes (R₂SiH₂) provide either dinuclear complexes with bridging μ-SiR₂ groups or mononuclear species containing a M–SiHR₂ unit depending upon the steric bulk of the groups at silicon.¹

A number of dinuclear Pt₂Si₂ complexes containing bridging silylene groups are known (C, Chart 1), and several of these compounds have been structurally characterized by X-ray crystallography. Tessier and co-

Chart 1



workers prepared a number of ring systems of type C (Chart 1) from reaction of RSiH₃ with (Et₃P)₂PtCl₂ in the presence of 2 equiv of Na metal (R = phenyl, *p*-tolyl, cyclohexyl).² Recently, they have examined the reaction of (R₃P)₃Pt (R = Et, Pr) with (Hex)SiH₃ and observed the formation of two different types of disilaplatacyclics, $\{[(\text{R}_3\text{P})_2\text{Pt}[\mu\text{-SiH}(\text{Hex})]]_2$ and $\{(\text{R}_3\text{P})\text{Pt}[\mu\text{-}\eta^2\text{-HSi}[\text{Pt}(\text{PR}_3)_2\text{H}](\text{Hex})]]_2$ depending upon the reaction conditions.³ Tilley's group has also generated several Pt₂Si₂ metallacycles from reaction of RSiH₃ (R = Ph, *p*-Tol, and Mes) with (Et₃P)₃Pt when a 2:1 ratio of Pt:Si precursors are used or from a 1:1 ratio of (Et₃P)₂Pt-(SiH₂Ar)₂ with Pt(PEt₃)₃.⁴ In addition, they observed the formation of an unusual dinuclear Pt–Si complex.⁴ Fink and Michalczyk reacted disilane (H₃Si–SiH₃) and 1,2-dimethyldisilane (MeH₂Si–SiH₂Me) with (dcpe)PtH₂ [dcpe = 1,2-bis(dicyclohexylphosphino)ethane] and observed the formation of some novel platinum silyl complexes including the disiladiplatinacycle [(dcpe)Pt-(μ-SiHR)]₂ (R = H, Me).⁵ Tanaka et al. examined the reactivity of 1,2-disilylbenzene with (Et₃P)₃Pt.⁶ Different products were formed depending upon the reaction conditions. When a 1:1 ratio of 1,2-bis(SiH₃)₂C₆H₄ and (Et₃P)₃Pt was used, quantitative formation of a novel mixed valence Pt^{II}Pt^{IV}Si₄P₄ disiladiplatinacycle was observed. A recent review has summarized the chem-

[†] Corresponding author. Tel: (314) 516-6436. Fax: (314) 516-5342. E-mail: jwilking@umsl.edu.

(1) (a) Corey, J. Y.; Braddock-Wilking, J. *Chem. Rev.* **1999**, *99*, 175. (b) Tilley, T. D. In *The Silicon Heteroatom Bond*; Patai, S., Rappoport, Z., Eds.; John Wiley and Sons: New York, 1991; p 245. (c) Tilley, T. D. In *The Chemistry of Organic Silicon Compounds*; Patai, S., Rappoport, Z., Eds.; John Wiley and Sons: New York, 1989; p 1416. (d) Aylett, B. J. *Adv. Inorg. Chem. Radiochem.* **1982**, *25*, 1.

(2) (a) They also found that reaction of Ph₂SiHLi and (PEt₃)₂PtCl₂ afforded dinuclear Pt₂Si₂ ring systems as cocrystallized mixtures: Zarate, E. A.; Tessier-Youngs, C. A.; Youngs, W. J. *J. Am. Chem. Soc.* **1988**, *110*, 4068. (b) Tessier, C. A.; Kennedy, V. O.; Zarate, E. A. In *Inorganic and Organometallic Oligomers and Polymers: Proceedings of the 33rd IUPAC Symposium on Macromolecules*; Harrod, J. F., Laine, L. M., Eds.; Kluwer Academic: Boston, MA, 1991; p 13. (c) Zarate, E. A.; Tessier-Youngs, C. A.; Youngs, W. J. *J. Chem. Soc., Chem. Commun.* **1989**, 577. (d) Anderson, A. B.; Shiller, P.; Zarate, E. A.; Tessier-Youngs, C. A.; Youngs, W. J. *Organometallics* **1989**, *8*, 2320.

(3) Sanow, L. M.; Chai, M.; McConnell, D. B.; Galat, K. J.; Simons, R. S.; Rinaldi, P. L.; Youngs, W. J.; Tessier, C. A. *Organometallics* **2000**, *19*, 192.

(4) Heyn, R. H.; Tilley, T. D. *J. Am. Chem. Soc.*, **1992**, *114*, 1917.

(5) Michalczyk, M. J.; Calabrese, J. C.; Recatto, C. A.; Fink, M. J. *J. Am. Chem. Soc.* **1992**, *114*, 7955.

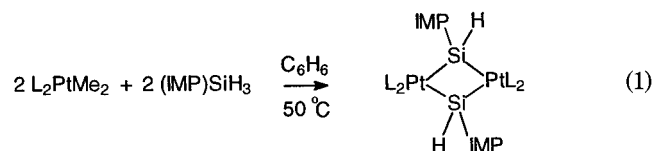
(6) Shimada, S.; Tanaka, M.; Honda, K. *J. Am. Chem. Soc.* **1995**, *117*, 8289.

istry of complexes containing bridging SiR₂ and GeR₂ ligands.⁷ These types of complexes are of importance since platinum complexes containing both mono- and bis(silyl) groups are believed to play a role in dehydrocoupling⁸ and hydrosilylation⁹ reactions.

Dinuclear platinum complexes containing bridging silylene groups and bridging hydrides (Pt...H...Si) are also known (**D**, Chart 1).^{3,10,11,12} Recently, we prepared complexes of the formula [(Ph₃P)Pt(μ - η^2 -H-SiHAr)]₂ from reaction of bulky arylsilanes (ArSiH₃) with (Ph₃P)₂Pt(η^2 -C₂H₄).^{11,12} In our quest to understand the mechanistic details involved in the formation of these complexes, we examined how steric and/or electronic factors associated with the metal precursor influence their formation. Herein, we report the study of reactions of platinum complexes of the type (Ph_{*n*}Me_{3-*n*}P)₂PtMe₂ (*n* = 0–2) with the sterically demanding arylsilane (IMP)SiH₃ (**1**, IMP = 2-isopropyl-6-methylphenyl),¹² which provided complexes {(Ph_{*n*}Me_{3-*n*}P)₂Pt[μ -SiH(IMP)]₂} [*n* = 0 (**2**), 1 (**3**), 2 (**4**)]. The platinum precursors utilized in the current study contain a series of phosphines which differ in both steric requirements (cone angles range from 118° to 136°) and basicity (p*K*_a's range from 8.65 to 4.57).

Results and Discussion

Reaction of (Ph_{*n*}Me_{3-*n*}P)₂PtMe₂ (*n* = 0–2) in a 1:1 ratio with the sterically hindered silane (IMP)SiH₃, **1**, afforded the dinuclear complexes **2–4** (eq 1) exclusively as the trans isomers in yields of 20–30%. Complex **4**



L = PMe₃ (**2**), PMe₂Ph (**3**), PMePh₂ (**4**)

was generated in 70% yield using the platinum precursor Pt(PMePh₂)₄, but the reaction was slow.¹³ Compounds **2–4** appear to be air stable both in solution and in the solid and were characterized by ¹H, ¹H{³¹P}, ³¹P{¹H}, and ²⁹Si{¹H} (**3** only) NMR spectroscopy, IR, X-ray crystallography, and elemental analyses. Selected spectroscopic data are shown in Table 1.

The ¹H NMR spectra for complexes **2–4** exhibit a complex multiplet for the Si–H resonance due to coupling to ³¹P and ¹⁹⁵Pt nuclei in the region 5.35–5.80 ppm. Upon decoupling of the ³¹P nuclei, the multiplet

Table 1. Selected NMR Data for Complexes 2–4

	¹ H (SiH) ^a	³¹ P{ ¹ H} ^a
[(Me ₃ P) ₂ Pt(μ -SiH(IMP)) ₂ , 2	5.35 <i>J</i> = 27 ^b	–13.8 <i>J</i> = 1693 ^c <i>J</i> = 266 ^d <i>J</i> = 21 ^e
[(PhMe ₂ P) ₂ Pt(μ -SiH(IMP)) ₂ , 3	5.79 <i>J</i> = 169 ^f <i>J</i> = 30 ^b	–2.1 <i>J</i> = 1725 ^c <i>J</i> = 271 ^d <i>J</i> = 20 ^e
[(Ph ₂ MeP) ₂ Pt(μ -SiH(IMP)) ₂ , 4	5.80 <i>J</i> = 36 ^b	13.5 <i>J</i> = 1793 ^c <i>J</i> = 287 ^d <i>J</i> = 39 ^e

^a Chemical shift given in ppm, coupling constants in Hz, data collected in C₆D₆ solvent. ^b ²*J*_{PtH}. ^c ¹*J*_{PtP}. ^d ³*J*_{PtP}. ^e ⁴*J*_{PP}. ^f ¹*J*_{SiH}.

collapses to a single line flanked by Pt satellites. Due to the low solubility of **2–4**, it was only possible to observe the Si satellites in compound **3**. The Si–H coupling in **3** was ¹*J*_{SiH} = 160 Hz, lower than that observed in the starting silane **1** [¹*J*_{SiH} = 200 Hz]. This observation is consistent with an expected decrease in the magnitude of the Si–H coupling in a metal-coordinated silyl complex relative to the free silane.¹ The ¹H NMR data for **2–4** are in good agreement with those reported by Tessier et al. for {(Pr₃P)₂Pt[μ -SiH(Hex)]₂}, which exhibited a ¹H NMR resonance at 3.89 ppm for the trans isomer (¹*J*_{SiH} = 159 Hz) and 3.54 ppm for the cis isomer.³

The P–CH₃ resonances appeared in the expected region in the ¹H NMR spectrum near 1.1 ppm, and a single resonance was found for compounds **2** and **4**. However, two P–CH₃ resonances were found for complex **3**, with two slightly different ³*J*_{PtH} coupling constants (20 and 23 Hz). These resonances couple equally to the ³¹P nuclei, as observed from a ¹H–³¹P COSY experiment. No change was observed in the ¹H{³¹P} NMR spectrum for **3** upon heating to 105 °C. The presence of two PMe₂Ph resonances in **3** might be explained on the basis of a hindered rotation of the Me groups around the P center. Since the presence of π -stacking between the phenyl groups on adjacent phosphorus atoms is strongly suggested in **3** in the solid state (see below), it is plausible that the interaction is also favorable in solution.

The ³¹P{¹H} NMR spectra for **2–4** exhibit part of an AA'A''XX' spin system. Complexes **2** and **3** show the expected resonances associated with a symmetrical dinuclear species containing one ¹⁹⁵Pt nucleus, i.e., four sets of pseudotriplets centered around a main central peak (Figure 1 shows spectrum for **2**). Compound **4** exhibits some unusual features and is discussed in detail below. It was possible to resolve only two peaks for the case where both ¹⁹⁵Pt nuclei are present (11.4%) due to low solubility. The chemical shifts for the phosphorus resonance in **2–4** appear successively downfield from –13 to +13 ppm with increasing Ph substitution on the phosphine. The values of ¹*J*_{PtP} coupling constants for **2–4** (1684, 1720, and 1793 Hz, respectively) are consistent with a species that has phosphorus atoms in a cis arrangement and one that contains a ligand that has a strong trans influence (silicon) at the Pt center. These values fall in the range observed for other P₂Pt(μ -SiR₂)₂ ring structures (i.e., ¹*J*_{PtP} for {(R₃P)₂Pt[μ -SiH(Hex)]₂} was 1744 Hz).³ Additionally, the values

(7) Ogino, H.; Tobita, H. *Adv. Organomet. Chem.* **1998**, *42*, 223.

(8) (a) Gauvin, F.; Harrod, J. F.; Woo, H. G. *Adv. Organomet. Chem.* **1998**, *42*, 363. (b) Yamashita, H.; Tanaka, M. *Bull. Chem. Soc. Jpn.* **1995**, *68*, 403. (c) Tilley, T. D. *Acc. Chem. Res.* **1993**, *26*, 22. (d) Corey, J. Y. *Adv. Silicon Chem.* **1991**, *1*, 327. (e) Tilley, T. D. *Comm. Inorg. Chem.* **1990**, *10*, 37.

(9) *Comprehensive Handbook on Hydrosilylation*; Marciniak, B., Ed.; Pergamon Press: Oxford, U.K., 1992.

(10) Auburn, M.; Ciriano, M.; Howard, J. A. K.; Murray, M.; Pugh, N. J.; Spencer, J. L.; Stone, F. G. A.; Woodward, P. *J. Chem. Soc., Dalton Trans.* **1980**, 659.

(11) Braddock-Wilking, J.; Levchinsky, Y.; Rath, N. P. *Organometallics* **2000**, *19*, 5500.

(12) Levchinsky, Y.; Rath, N. P.; Braddock-Wilking, J. *Organometallics* **1999**, *18*, 2583.

(13) Slow dissociation of PMePh₂ from the platinum precursor which probably accounts for a slow reaction with the silane. Clark, H. C.; Itoh, K. *Inorg. Chem.* **1971**, *10*, 17.

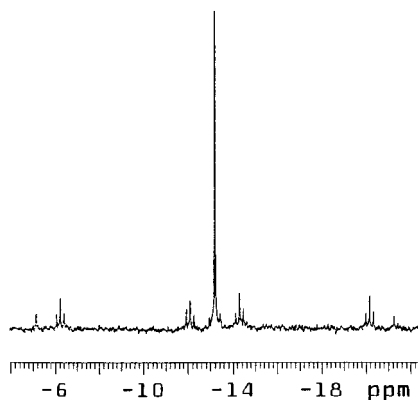


Figure 1. $^{31}\text{P}\{^1\text{H}\}$ NMR spectrum of **2** (121 MHz, C_6D_6).

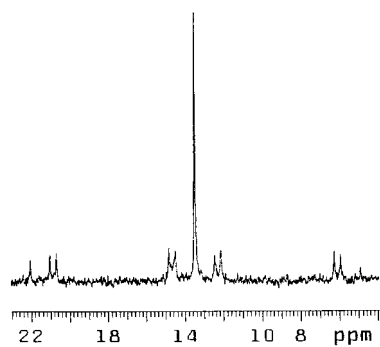


Figure 2. $^{31}\text{P}\{^1\text{H}\}$ NMR spectrum of **4** (121 MHz, C_6D_6).

of $^1J_{\text{PtP}}$ decrease as the basicity of the phosphine increases and the cone angle decreases. This was a surprising observation considering the fact that, in general, the values of $^1J_{\text{PtP}}$ decrease as the steric requirements of the phosphine ligands increase.¹⁴ On the other hand, Grim and associates found that $^1J_{\text{WP}}$ couplings decrease as the basicity of the phosphine ligands increases.¹⁵

While the solid-state structure of **4** (see below) showed two phosphine ligands at each platinum center, the satellite pattern in the $^{31}\text{P}\{^1\text{H}\}$ NMR spectrum (Figure 2) of **4** was consistent with the presence of only one phosphine and can be described as a part of an AA'XX' spin system. The $^{31}\text{P}\{^1\text{H}\}$ NMR and $^1\text{H}\{^{31}\text{P}\}$ NMR spectra for an analytically pure sample of **4** indicated the presence of free phosphine, which appeared as a broad resonance. Cooling the sample to -90°C had no effect on the spectrum, even though it was not possible to see the free phosphine at lower temperatures. The most likely reason for phosphine dissociation is due to steric effects associated with a small P–Pt–P angle.

The observation of phosphine dissociation from each Pt center in **4** strongly suggests that the PMePh_2 ligand ($\theta = 136^\circ$) defines the upper limit of steric capacity at platinum in complexes of the type $\{[(\text{R}_3\text{P})_2\text{Pt}][\mu\text{-SiHAr}]\}_2$ (Ar = IMP, or any other bulky aryl group).¹¹ In fact, reaction of $(\text{Ph}_3\text{P})_2\text{PtMe}_2$ (cone angle for $\text{Ph}_3\text{P} = 145^\circ$)¹⁴ with $(\text{IMP})\text{SiH}_3$ did not generate $\{(\text{Ph}_3\text{P})_2\text{Pt}[\mu\text{-SiH}(\text{IMP})]\}_2$ analogous to **2–4** but instead gave a dinuclear complex containing bridging silylene groups and bridging hydrides, $\{(\text{Ph}_3\text{P})\text{Pt}[\mu\text{-}\eta^2\text{-H-SiH}(\text{IMP})]\}_2$.¹⁶ However, a possibility still exists that the basicity of

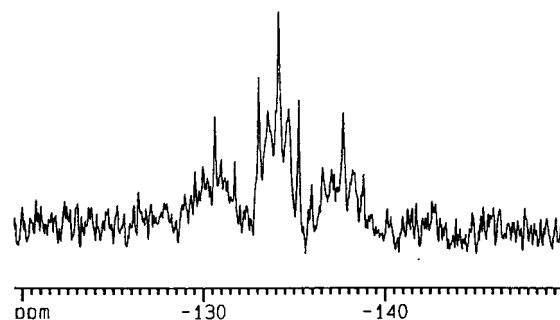


Figure 3. $^{29}\text{Si}\{^1\text{H}\}$ DEPT NMR spectrum of **3** (99 MHz, C_6D_6).

the phosphine ligands on the Pt center could be an important factor, as PPh_3 is also less basic (e.g., $\text{p}K_{\text{a}}$ for $\text{PPh}_3 = 2.73$, $\text{p}K_{\text{a}}$ for $\text{PMePh}_2 = 4.57$).

The ^{29}Si NMR spectrum¹⁷ of **3** showed two sets of overlapping triplets centered at -134 ppm flanked by Pt satellites ($^1J_{\text{SiPt}} = 699$ Hz) (Figure 3). This is a significant shift compared to the value of the silane precursor **1**, which appears at -77 ppm.¹² In general, the chemical shift for a metal-bound silyl group moves to low field compared to the parent hydrosilane.¹⁷ The multiplicity pattern is due to inequivalent coupling of cis and trans phosphines to the Si center [$^2J_{\text{PSi}} = 66$ Hz (cis), $^2J_{\text{PSi}} = 107$ Hz (trans)]. The platinum satellites appear as an overlapping pseudo triplet of triplets and are due to the inequivalency between four phosphorus nuclei when one of the Pt nuclei is NMR active. Thus, four sets of overlapping satellite doublets would be expected.

The high-field value for the ^{29}Si resonance for **3** (and a related system prepared by Tessier et al., see below) is unusual since the recent review by Ogino and Tobita summarized the ^{29}Si chemical shift range for most bridging silylene moieties in transition metal complexes (including those with $\text{M}\cdots\text{H}\cdots\text{Si}$ interactions) as $+60$ to $+290$ ppm.⁷ Dinuclear complexes containing a bridging silylene group without a metal–metal bond generally exhibit ^{29}Si resonances in the region 60 – 160 ppm, and those that contain a hydrogen bridging the metal–silylene bond ($\text{M}\cdots\text{H}\cdots\text{Si}$ interaction) appear between 85 and 165 ppm.⁷ A low-field shift of >200 ppm is often observed for bridging silylene complexes containing a metal–metal bond with the general formula $\text{Cp}_2\text{Fe}_2(\text{CO})_2(\mu\text{-CO})(\mu\text{-SiR}_2)$.⁷

In contrast, the ^{29}Si signal for $\{(\text{Ph}_3\text{P})\text{Pt}[\mu\text{-}\eta^2\text{-H-SiH}(\text{IMP})]\}_2$ was found ca. $+130$ ppm with a substantially larger coupling to Pt ($^1J_{\text{PtSi}} = 1527$ Hz).^{11,12} Therefore, two platinum silyl dimers containing the same Si substituents and slightly different phosphine ligands were found to have ^{29}Si chemical shifts that span a range of ~ 260 ppm! This trend was also observed in the related systems $\{(\text{Et}_3\text{P})_2\text{Pt}[\mu\text{-SiH}(\text{Hex})]\}_2$ and $\{(\text{R}_3\text{P})\text{Pt}[\mu\text{-}\eta^2\text{-H-Si}[\text{Pt}(\text{PR}_3)_2\text{H}](\text{Hex})]\}_2$,² which exhibited ^{29}Si resonances at -66 ppm (cis, $^1J_{\text{PtSi}} = 676$ Hz), -93 (trans, $^1J_{\text{PtSi}} = 667$ Hz), and $+194$ ppm ($^1J_{\text{PtSi}} = 707$ Hz), respectively.³

(16) Braddock-Wilking, J.; Levchinsky, Y. Unpublished results. See ref 11 for synthesis and characterization of $\{(\text{R}_3\text{P})\text{Pt}[\mu\text{-}\eta^2\text{-H-SiH}(\text{Ar})]\}_2$.

(17) For a recent review on NMR spectroscopy of organosilicon compounds see for example: Williams, E. A. In *The Chemistry of Organic Silicon Compounds*, Part 1; Patai, S., Rappaport, Z., Eds.; John Wiley & Sons: New York, 1989; Chapter 8.

(14) Tolman, C. A. *Chem. Rev.* **1977**, *77*, 313.

(15) Grim, S. O.; Wheatland, D. A.; McFarlane, W. J. *Am. Chem. Soc.* **1967**, *89*, 5573.

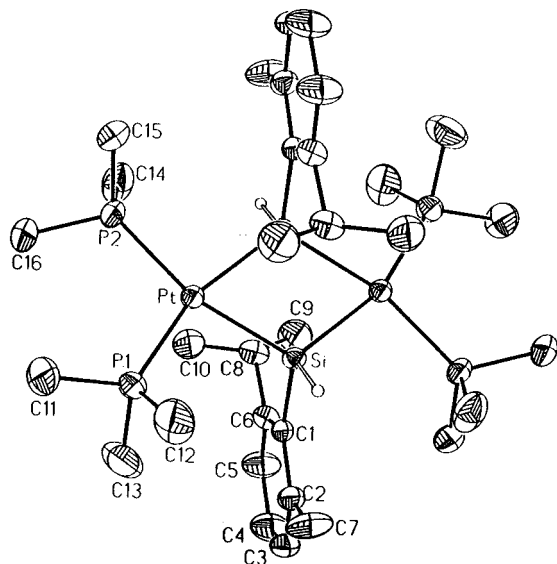


Figure 4. Molecular structure of $\{(Me_3P)_2Pt[\mu-SiH(IMP)]\}_2$, **2**, with thermal ellipsoids drawn at 50% probability. Hydrogen atoms (except Si–H) have been omitted for clarity.

The Si–H stretching frequency of **2–4** appeared in the infrared region between 2021 and 2054 cm^{-1} . These values are in good agreement with those reported by Tessier et al. for $\{(R_3P)_2Pt[\mu-SiH(Hex)]\}_2$ (R = Et, $\nu(Si-H) = 1985\text{ cm}^{-1}$; R = Pr, $\nu(Si-H) = 1984\text{ cm}^{-1}$).³

The reaction of **1** with $(PhMe_2P)_2PtMe_2$ was monitored by 1H , $^{29}Si\{^1H\}$, and $^{31}P\{^1H\}$ NMR spectroscopy. Both the 1H and ^{31}P NMR spectra of the reaction mixture indicated the presence of two new platinum-containing products (one of them corresponding to **3**). The second platinum-containing complex was assigned to the bis(silyl) species $(PhMe_2P)_2Pt[SiH_2(IMP)]_2$, **6**. Complex **6** was not isolated and could not be separated from unreacted $(PhMe_2P)_2PtMe_2$. These results are consistent with those reported by Tilley et al., who observed the formation of Pt_2Si_2 dimers from bis(silyl) platinum intermediates with $Pt(PET_3)_3$.⁴

In addition, 1H and ^{29}Si NMR spectroscopy (as well as GC–MS analysis) of the reaction mixture showed the presence of an organosilane which was assigned to $(IMP)SiH_2Me$.¹⁸ The formation of this compound suggests that oxidative addition of a Si–H bond in $(IMP)SiH_3$ to the Pt center could occur to give a Pt(IV) complex¹⁹ with the composition $(Ph_nMe_{3-n}P)_2Pt(H)(Me)_2[SiH_2(IMP)]$. This species could reductively eliminate $MeSiH_2(IMP)$ (or CH_4) followed by reaction with a second equivalent of $(IMP)SiH_3$ to give the bis(silyl) complex. The generation of a Pt(IV) species is consistent with the report by Fink and Michalczuk, who observed the formation of *fac*-(dcpe)Pt(SiMeHSiMeH₂)H₃ by low-temperature NMR spectroscopy from the reaction of (dcpe)PtH₂ with H₂MeSiSiMeH₂.⁵ An alternative mechanism would involve a metathesis reaction between $(R_3P)_2PtMe_2$ and $(IMP)SiH_3$, which could also generate $(IMP)SiH_2Me$.

(18) GC–MS, 1H NMR, and $^{29}Si\{^1H\}$ NMR spectroscopic data are analogous to an authentic sample prepared from $(IMP)MgBr + MeSiHCl_2$ followed by $LiAlH_4$ reduction. Braddock-Wilking, J. Unpublished results.

(19) Eaborn et al. suggested the formation of Pt(IV) species from reaction of P_2PtMe_2 with some secondary and tertiary hydrosilanes. Eaborn, C.; Pidcock, A.; Ratcliff, B. *J. Organomet. Chem.* **1974**, *66*, 23.

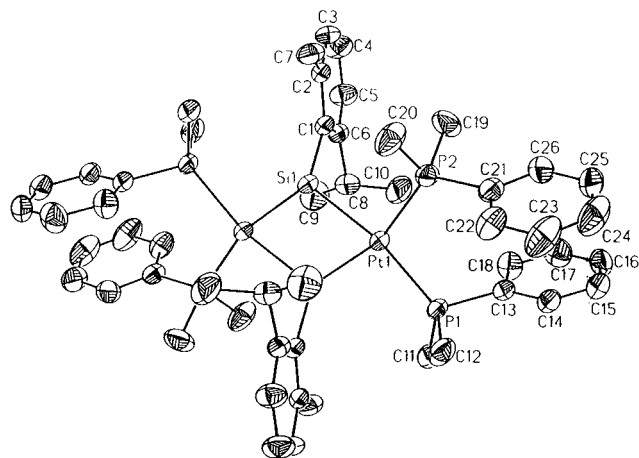


Figure 5. Molecular structure of $\{(PhMe_2P)_2Pt[\mu-SiH(IMP)]\}_2$, **3**, with thermal ellipsoids drawn at 50% probability. Hydrogen atoms (except Si–H) have been omitted for clarity.

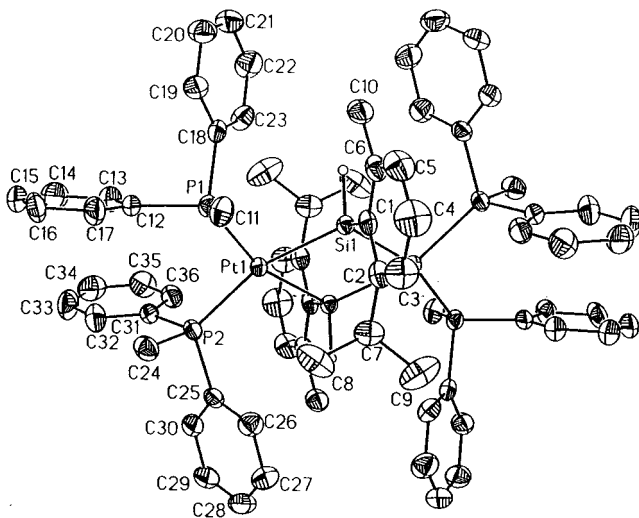


Figure 6. Molecular structure of $\{(Ph_2MeP)_2Pt[\mu-SiH(IMP)]\}_2$, **4**, with thermal ellipsoids drawn at 50% probability. Hydrogen atoms (except Si–H) have been omitted for clarity.

X-ray Crystallographic Study of 2–4. Compounds **2–4** were structurally characterized by X-ray crystallography, and the molecular structures are shown in Figures 4–6, respectively. Crystallographic data and structural refinement data for **2–4** are given in Table 2, and selected bond distances and angles for **2–4** and related derivatives are in Table 3. As a general trend, complexes **2–4** were found to exhibit a planar diamond shaped Pt_2Si_2 core with the IMP groups lying directly above and below the central ring. The hydrogen atoms on Si were located and refined in complexes **2** and **3**. One notable feature found in **2–4** as well as related Pt_2Si_2 ring systems is the Si...Si separation.^{2,3} These distances fall in the upper range of known Si–Si single-bond distances (2.33–2.70 Å).²⁰ Theoretical studies have suggested a $\mu_2-\eta^2$ -disilene type geometry for the model

(20) For a comparison of reported bond distances of Si–X see for example: (a) Klebe, G. *J. Organomet. Chem.* **1985**, *293*, 147. (b) Corey, J. Y. In *The Chemistry of Organic Silicon Compounds*, Part 1; Patai, S., Rappaport, Z., Eds.; John Wiley & Sons: New York, 1989; Chapter 1. (c) Sheldrick, W. S. In *The Chemistry of Organic Silicon Compounds*, Part 1; Patai, S., Rappaport, Z., Eds.; John Wiley & Sons: New York, 1989; Chapter 3.

Table 2. Crystal Data and Structure Refinement for 2–4

	2	3	4
formula	C ₁₆ H ₃₂ P ₂ PtSi	C ₅₂ H ₇₂ P ₂ Pt ₂ Si ₂	C ₄₂ H ₄₆ P ₂ PtSi
fw	509.54	1267.34	835.91
temperature (K)	293(2)	223(2)	223(2)
cryst dimens (mm)	0.22 × 0.20 × 0.20	0.28 × 0.22 × 0.14	0.34 × 0.30 × 0.22
cryst syst	triclinic	triclinic	triclinic
space group	<i>P</i> 1	<i>P</i> 1	<i>P</i> 1
<i>a</i> (Å)	9.7269(1)	9.2786(1)	12.5935(1)
<i>b</i> (Å)	10.9682(1)	12.0407(1)	12.7862(1)
<i>c</i> (Å)	11.0411(1)	12.922(1)	14.1237(1)
α (deg)	111.026(1)	84.338(1)	94.051(1)
β (deg)	109.503(1)	72.68(1)	116.342(1)
γ (deg)	93.665(1)	71.10(1)	109.575(1)
<i>V</i> (Å ³)	1013.58(2)	1303.94(2)	1854.39(2)
<i>Z</i>	2	1	2
<i>d</i> _{calc} (mg/m ³)	1.670	1.614	1.497
μ (mm ⁻¹)	7.130	5.560	3.930
GOF	1.118	1.016	1.022
R1 (obsd data)	0.0298	0.0282	0.0292
wR2 (all data)	0.0684	0.0538	0.0641
largest diff peak (e Å ⁻³)	1.215	1.517	1.756

Table 3. Selected Bond Lengths [Å] and Angles [deg] for 2–4 and Related Compounds

	2	3	4	(R ₃ P) ₂ Pt- (μ-SiR'R'') ₂ ^{2,3}
Bond Distances				
Pt–P1	2.3215(13)	2.3124(9)	2.3306(8)	
Pt–P2	2.3164(13)	2.3163(10)	2.3397(8)	
Pt–Si	2.4054(12)	2.4039(8)	2.4089(9)	2.355–2.408
Pt–Si#1	2.4087(12)	2.4006(10)	2.4070(8)	
Pt···Pt	4.004	3.962	4.030	3.973–4.046
Si···Si#1	2.673(2)	2.718(2)	2.637(2)	2.554–2.612
Bond Angles				
Si–Pt–Si#1	67.46(5)	68.89(4)	66.40(3)	64.4–66.6
Pt–Si–Pt#1	112.54(5)	111.11(4)	113.60(3)	112.6–115.5
P1–Pt–Si	94.67(4)	164.10(3)	95.83(3)	
P1–Pt–Si#1	160.59(5)	95.80(3)	161.77(3)	
P2–Pt–Si	160.44(4)	94.59(3)	162.35(3)	
P2–Pt–Si#1	94.34(4)	162.81(3)	98.92(3)	
P2–Pt–P1	104.24(5)	100.99(3)	99.28(3)	
Pt–Si–Si#1	56.33(4)	55.50(3)	56.76(3)	
Pt#1–Si–Si#1	56.21(4)	55.61(3)	56.83(3)	

compound *trans*-Pt₂(PH₃)₄(SiPhCl)₂, where the Si–Si Mulliken overlap was 0.27.^{2d} The Pt···Pt nonbonding distances in **2–4** and these related Pt₂Si₂ ring systems^{2,3} are 3.9–4.0 Å (van der Waals radius of Pt²¹ 1.7–1.8 Å). The Pt–Si bond lengths in **2–4** (~2.4 Å) are found at the higher end of the range for Pt–Si distances (2.25–2.44 Å)¹ and are similar to those reported by Tessier for related complexes.^{2,3}

A prominent feature found in **2–4** and related Pt₂Si₂ ring systems are acute Si–Pt–Si and obtuse Pt–Si–Pt angles. The Si–Pt–Si angles for **2–4** range from 66° to 69°, but the related complexes prepared by Tessier show slightly smaller angles.^{2,3} The Pt–Si–Pt angles for **2–4** and Tessier's complexes^{2,3} (*trans* isomers) fall in the range 111–116°. These Pt₂Si₂ systems display ring structures opposite the complexes [(R₃P)Pt(μ-η²-H–SiHR')]₂, which possess bridging hydrides (Pt···H···Si). The latter systems exhibit acute Pt–Si–Pt angles, obtuse Si–Pt–Si angles, Pt–Pt bonds, and long Si···Si separations.^{3,10,11,12}

Examination of the ring environment in **2–4** reveals some unusual features. It is reasonable to expect the following changes in the key angles P2–Pt–Si (in-

crease), Pt–Si–Pt (increase), Si–Pt–Si (decrease) and an increase in the Pt–P bond length, as the phosphine becomes more sterically demanding. The steric bulk of the phosphines increases on going from **2** → **4** [cone angle for the PMe₂Ph ligand (122°) lies between PMe₃ (118°) and PMePh₂ (136°)]. The Si–Pt–Si angles in **3** are significantly higher than the corresponding angles in **2** and **4**, while the value of the Pt–Si–Pt angle in **3** is smaller. Furthermore, the Si···Si distance in **3** was found to be the longest (2.718 Å).²² These unusual observations might be explained by the presence of π-stacking interactions between the phenyl groups on the adjacent phosphine atoms. The plane-to-plane distance between the phenyl groups in **3** was calculated to be 3.97 Å. Although this distance is long, π-stacking may account for the greater solubility of **3** in aromatic solvents (as opposed to **2** and **4**).

Conclusion

Dimeric (μ-silylene)platinum species of the type {(R₃P)₂Pt}[μ-SiH(IMP)]₂ (**C**, Chart 1) were obtained from reaction of (IMP)SiH₃, **1**, with a series of Pt(II) phosphine complexes. Despite the difference in the basicity and the steric requirements of the phosphine ligands on the starting platinum material, complexes **2–4** exhibit similar structural features, as determined by NMR spectroscopy and X-ray crystallography. In addition, complex **4** (containing the most sterically hindered phosphine, PMePh₂) was found to undergo dissociation of one of the phosphine ligands at each Pt center in solution. This suggests that reaction of **1** with other platinum precursors containing phosphine ligands with a cone angle of greater than 136° should give a Pt–Si product of the type {(Ph₃P)Pt[μ-η²-H–SiH(Ar)]₂ (**D**, Chart 1).^{11,12} Thus, it appears that steric constraints with respect to the substituents at Pt have a significant impact on the nature of the product formed.

In a previous paper we reported that bulky groups at silicon (RSiH₃) provided compounds of type **A** or **D** (Chart 1). However, less sterically demanding primary silanes generally produced bis(silyl) complexes analogous to **B**. The current study has demonstrated that the

(21) Huheey, J. E. *Inorganic Chemistry*, 3rd ed.; Harper & Row: New York, 1983.

(22) The Si···Si distance in **3** represents the longest separation among structurally characterized dimers of this type.

nature of the phosphine in the platinum precursor influences the nature of the product formed (using the same silane precursor). In addition, the stronger coordinating ability of basic phosphines to a metal center could be important in the dissociation of the phosphine, which is required for the formation of complexes of the type $[(\text{Ph}_3\text{P})\text{Pt}(\mu\text{-}\eta^2\text{-H-SiHAr})_2]$. A study of the influence of electronic effects associated with groups at silicon and platinum on the formation of dinuclear Pt_2Si_2 complexes is in progress.

Experimental Section

General Materials and Procedures. All reactions and manipulations were performed in dry glassware under an argon atmosphere in an inert atmosphere drybox or on a double manifold Schlenk line. ^1H and ^{31}P NMR data were obtained on a Varian Unity Plus 300 MHz WB spectrometer or a Bruker ARX-500 MHz spectrometer (ambient and variable temperatures) using a 5 mm tunable broadband probe. ^{29}Si NMR data were collected on a Bruker ARX-500 MHz spectrometer. NMR experiments were performed in C_6D_6 , CD_2Cl_2 , or toluene- d_6 , and chemical shifts are reported relative to residual protonated solvent. Phosphorus chemical shifts are reported relative to external H_3PO_4 (0 ppm). $^{29}\text{Si}\{^1\text{H}\}$ NMR data were collected using the DEPT sequence²³ at room temperature and are reported relative to external TMS (0 ppm). Infrared spectra were recorded on a Perkin-Elmer 1600 Series FT-IR (as KBr pellets). X-ray crystal structure determinations were performed on a Bruker SMART diffractometer equipped with a CCD area detector at 223 K. Elemental analyses were obtained from Atlantic Microlab, Inc., Norcross, GA.

Pentane and benzene were distilled over CaH_2 . Diethyl ether and 1,2-dimethoxyethane were distilled from sodium/benzophenone ketyl. Solvents were degassed by standard methods before they were taken into the drybox. Toluene- d_6 , CD_2Cl_2 , and C_6D_6 were dried over activated alumina (neutral) or Lindle catalyst before use. The platinum (phosphine) complexes Me_2PtL_2 ($\text{L} = \text{PMe}_3$, PMe_2Ph , PMePh_2) were prepared according to the literature procedures.²⁴ $\text{Pt}(\text{PMePh}_2)_4$ was prepared in a manner similar to $\text{Pt}(\text{PPh}_3)_4$.²⁵ The synthesis of $(\text{IMP})\text{SiH}_3$, **1**, was previously reported.¹²

Synthesis of $\{[(\text{Me}_3\text{P})_2\text{Pt}][\mu\text{-SiH(IMP)}]\}_2$ (2**).** A solution of $(\text{IMP})\text{SiH}_3$, **1** (57 mg, 0.35 mmol), in 1 mL C_6H_6 was added to a solution of $(\text{Me}_3\text{P})_2\text{PtMe}_2$ (130 mg, 0.35 mmol, 1.5 mL C_6H_6), resulting in a pale yellow mixture. The pale yellow solution was heated to 50 °C for 21 h, and the color changed from pale yellow to bright orange. Addition of Et_2O (2 mL) to the reaction mixture followed by cooling at -35 °C resulted in the formation of orange microcrystals of $\{[(\text{Me}_3\text{P})_2\text{Pt}][\mu\text{-SiH(IMP)}]\}_2$, **2** (38 mg, 22%). Crystals of **2** suitable for an X-ray analysis were obtained by slow evaporation of a C_6D_6 solution at room temperature.

$^1\text{H}\{^{31}\text{P}\}$ NMR (C_6D_6 , 300 MHz): δ 1.09 (s, 36H, $^3J_{\text{PtH}} = 20$ Hz, $\text{P}(\text{CH}_3)_3$), 1.43 (d, 12H, $^3J_{\text{HH}} = 7$ Hz, $\text{ArCH}(\text{CH}_3)_2$), 3.07 (s, 6H, ArCH_3), 4.46 (bm, 2H, $\text{ArCH}(\text{CH}_3)_2$), ArH region 6.88–7.43 (6H). IR (KBr, cm^{-1}): ν 2024.0 (Si–H). Anal. Calcd for $\text{C}_{32}\text{H}_{64}\text{P}_4\text{Pt}_2\text{Si}_2$: C, 37.72; H, 6.33. Found: C, 37.72; H, 6.53.

Synthesis of $\{[(\text{PhMe}_2\text{P})_2\text{Pt}][\mu\text{-SiH(IMP)}]\}_2$ (3**).** A solution of $(\text{IMP})\text{SiH}_3$, **1** (49 mg, 0.30 mmol), in 1 mL C_6D_6 was added to $(\text{PhMe}_2\text{P})_2\text{PtMe}_2$ (150 mg, 0.30 mmol) to give a pale yellow solution. The reaction mixture was heated to 60 °C for 24 h, and rapid bubbling was observed for the first 3 h, along with a gradual color change from yellow to orange. The solution was layered with 15 mL of pentane and set aside

for 24 h. Yellow crystals of $\{[(\text{PhMe}_2\text{P})_2\text{Pt}][\mu\text{-SiH(IMP)}]\}_2$, **3** (suitable for X-ray analysis), were obtained in 26% yield (49 mg).

$^1\text{H}\{^{31}\text{P}\}$ NMR (C_6D_6 , 300 MHz): δ 1.12 (s, 24H, $^3J_{\text{PtH}} = 20$ Hz, 23 Hz, $\text{P}(\text{CH}_3)_2$), 2.62 (s, 6H, ArCH_3), 3.40 (d, 12H, $^3J_{\text{HH}} = 6$ Hz, $\text{ArCH}(\text{CH}_3)_2$), 4.81 (bm, 2H, $\text{ArCH}(\text{CH}_3)_2$), ArH region 6.87–7.33 (26H). $^{29}\text{Si}\{^1\text{H}\}$ NMR (C_6D_6 , DEPT, 99 MHz): δ -134.2 [m, $^1J_{\text{PtSi}} = 699$ Hz, $^2J_{\text{PSi}} = 66$ Hz (cis), $^2J_{\text{PSi}} = 107$ Hz (trans)]. ^1H – ^{31}P COSY NMR (500 MHz, C_7D_8): δ -2.1 (^{31}P resonance) showed cross-peak coupling to protons δ 1.11 (PCH_3), 1.35 (PCH_3), 5.73 (Si–H), 7.16 [$\text{o-PMe}_2(\text{C}_6\text{H}_5)$]. IR (KBr, cm^{-1}): ν 2021.4 (Si–H). Anal. Calcd for $\text{C}_{52}\text{H}_{72}\text{P}_4\text{Pt}_2\text{Si}_2$: C, 49.28; H, 5.73. Found: C, 49.38; H, 5.79.

Variable-Temperature NMR Spectroscopy of **3.** A sample of **3** (5 mg, 0.004 mmol) was dissolved in 1 mL of toluene- d_6 and analyzed by VT-NMR. The sample was analyzed by $^1\text{H}\{^{31}\text{P}\}$ NMR from room temperature (23 °C) to 90 °C in 10 deg increments to determine if a fluxional process was occurring between the two $\text{P}(\text{CH}_3)_2\text{Ph}$ resonances (1–2 ppm). No change was observed in the spectra over this temperature range, and no decomposition was found to take place after heating.

Synthesis of $\{[(\text{Ph}_2\text{MeP})_2\text{Pt}][\mu\text{-SiH(IMP)}]\}_2$ (4**).** A solution of $(\text{IMP})\text{SiH}_3$, **1** (24 mg, 0.15 mmol), in 1 mL of C_6D_6 was added to $(\text{Ph}_2\text{MeP})_2\text{PtMe}_2$ (83 mg, 0.13 mmol). The resulting pale yellow-brown solution was heated to 65 °C for 39 h. The reaction mixture was cooled to 0 °C, and Et_2O and pentane (20 mL, 50:50 mixture) were added. The solution was filtered, and the solid was dried in vacuo to afford $\{[(\text{Ph}_2\text{MeP})_2\text{Pt}][\mu\text{-SiH(IMP)}]\}_2$, **4**, as a bright yellow solid (30 mg, 30% yield). Crystals suitable for an X-ray analysis were obtained by slow evaporation of a C_6D_6 solution at room temperature. $^1\text{H}\{^{31}\text{P}\}$ NMR (C_6D_6 , 300 MHz): δ 1.51 (s, 6H, ArCH_3), 1.72 (s, 12H, $^3J_{\text{PtH}} = 24$ Hz, $\text{P}(\text{CH}_3)_2$), 1.89 (d, 12H, $^3J_{\text{HH}} = 6$ Hz, $\text{ArCH}(\text{CH}_3)_2$), 4.83 (bm, 2H, $\text{ArCH}(\text{CH}_3)_2$), ArH region 6.54–7.41 (46H). IR (KBr, cm^{-1}): ν 2054.0 (Si–H). Anal. Calcd for $\text{C}_{72}\text{H}_{80}\text{P}_4\text{Pt}_2\text{Si}_2\cdot\text{Et}_2\text{O}$: C, 57.37; H, 5.66. Found: C, 57.34; H, 5.62.

Alternative Preparation of **4 from $\text{Pt}(\text{PMePh}_2)_4$ and $(\text{IMP})\text{SiH}_3$ (**1**).** A sample of $\text{Pt}(\text{PMePh}_2)_4$ (125 mg, 0.082 mmol) was dissolved in 3 mL of C_6H_6 , and a solution of $(\text{IMP})\text{SiH}_3$, **1** (19 mg, 0.12 mmol, 1 mL of C_6H_6), was added to give a pale yellow mixture with mild gas evolution. After 24 h, additional C_6H_6 (3 mL) was added, and the reaction was heated to 50 °C for 24 h, during which the color changed from yellow to orange. After addition of pentane (7 mL) the reaction mixture was stored at -35 °C for 2 days, which resulted in the formation of large yellow crystals of **4**. The crystalline material was washed with DME (3×1 mL) and dried in vacuo, giving 67 mg (71%) of **4**. Spectroscopic data for **4** obtained from this route were identical to the data obtained from the $(\text{PMePh}_2)_2\text{PtMe}_2/(\text{IMP})\text{SiH}_3$ route.

Variable-Temperature NMR Spectroscopy of **4.** A sample of **4** (7 mg, 0.005 mmol) was dissolved in 1 mL of CD_2Cl_2 and analyzed by VT-NMR. The sample was analyzed by $^{31}\text{P}\{^1\text{H}\}$ NMR from room temperature (23 °C) to -90 °C in 10 deg increments to determine if a fluxional process was occurring. No change was observed in the $^{31}\text{P}\{^1\text{H}\}$ spectra over the temperature range studied. In addition, no free PMePh_2 was observed.

NMR Study of Reaction of **1 with $(\text{PhMe}_2\text{P})_2\text{PtMe}_2$.** The formation of the bis(silyl)platinum complex **6** was monitored by multinuclear NMR spectroscopy. Complex **6** was not isolated and thus was characterized in solution only. A description of the experiment is given for reaction of $(\text{PhMe}_2\text{P})_2\text{PtMe}_2$ with **1**. The analogous systems **5** and **7** are proposed on the basis of $^{31}\text{P}\{^1\text{H}\}$ NMR data.

$(\text{PhMe}_2\text{P})_2\text{PtMe}_2$ (66 mg, 0.13 mmol) and $(\text{IMP})\text{SiH}_3$, **1** (21 mg, 0.13 mmol), were placed in an NMR tube (sample prepared inside an inert atmosphere drybox). Benzene- d_6 (0.75 mL) was added, which gave a pale yellow solution. The sample was

(23) Blinka, T. A.; Helmer, B. J.; West, R. *Adv. Organomet. Chem.* **1984**, *23*, 193.

(24) Ruddick, J. D.; Shaw, B. L. *J. Chem. Soc. A* **1969**, 2801.

(25) Clark, H. C.; Itoh, K. *Inorg. Chem.* **1971**, *10*, 17.

heated at 60 °C for approximately 20 h. Analysis of the reaction mixture by ^1H , $^{29}\text{Si}\{^1\text{H}\}$, and $^{31}\text{P}\{^1\text{H}\}$ NMR spectroscopy revealed the formation of *cis*-(PhMe₂P)₂Pt[SiH₂(IMP)]₂, **6**, and $\{(\text{PhMe}_2\text{P})_2\text{Pt}[\mu\text{-SiH}(\text{IMP})]\}_2$, **3** (as well as unreacted (PhMe₂P)₂-PtMe₂).

Selected NMR data for 6: $^1\text{H}\{^{31}\text{P}\}$ NMR (C₆D₆, 500 MHz): δ 5.0 (s, 4H, $^1J_{\text{SiH}} = 172$ Hz, $^2J_{\text{PtH}} = 33$ Hz, SiH). $^{31}\text{P}\{^1\text{H}\}$ NMR (C₆D₆, 202 MHz): δ -7.3 ($^1J_{\text{PtP}} = 1773$ Hz). $^{29}\text{Si}\{^1\text{H}\}$ NMR (C₆D₆, 99 MHz): δ -51.8 (dd, $^1J_{\text{PtSi}} = 1075$ Hz, $^3J_{\text{PSi}} = 157$ Hz, $^3J_{\text{PSi}} = 21$ Hz).

Selected NMR data for 5: $^{31}\text{P}\{^1\text{H}\}$ NMR (C₆D₆, 121 MHz): δ -18.6 ($^1J_{\text{PtP}} = 1786$ Hz).

Selected NMR data for 7: $^{31}\text{P}\{^1\text{H}\}$ NMR (C₆D₆, 121 MHz): δ 10.1 ($^1J_{\text{PtP}} = 1801$ Hz).

In addition, an organosilane product was observed and was assigned the composition (IMP)MeSiH₂.¹⁸ Selected NMR data for (IMP)MeSiH₂: ^1H NMR (C₆D₆, 300 MHz): δ 4.65 (q, 2 H, SiH, $^1J_{\text{SiH}} = 192$ Hz, $^2J_{\text{SiH}} = 4.4$ Hz). $^{29}\text{Si}\{^1\text{H}\}$ NMR (C₆D₆, 99 MHz): δ -51.5 (s). GC-MS (EI, 70 eV): *m/z* 178 (30), 163 (11), 161 (24), 159 (22), 145 (10), 135 (28), 133 (100), 119 (14), 105 (25), 91 (10).

X-ray Crystallography for 2, 3, and 4. Crystals of appropriate dimensions were mounted on glass fibers in random orientations. Preliminary examination and data collection were performed using a Bruker SMART charge coupled device (CCD) detector system single-crystal X-ray diffractometer using graphite-monochromated Mo K α radiation ($\lambda = 0.71073$ Å) equipped with a sealed tube X-ray source. Preliminary unit cell constants were determined with a set of 45 narrow frames (0.3° in ω scans). A typical data set consists of 4028 frames of intensity data collected with a frame width of 0.3° in ω and counting time of 15 s/frame at a crystal-to-detector distance of 4.930 cm. The double pass method of scanning was used to exclude any noise. The collected frames were integrated using an orientation matrix determined from the narrow frame scans. SMART and SAINT software packages²⁶ were used for data collection and data integration. Analysis of the integrated data did not show any decay. Final cell constants were determined by a global refinement of *xyz* centroids of 8192 reflections. Collected data were corrected for

systematic errors using SADABS²⁷ based upon the Laue symmetry using equivalent reflections.

Crystal data and intensity data collection parameters are listed in Table 2.

Structure solution and refinement were carried out using the SHELXTL-PLUS software package.²⁶ The structures were solved by direct methods and refined successfully in the space group $P\bar{1}$ for all three crystals. Full-matrix least-squares refinements were carried out by minimizing $\sum w(F_o^2 - F_c^2)^2$. The non-hydrogen atoms were refined anisotropically to convergence. The terminal Si-H hydrogen atoms were located and refined freely. All other H atoms were treated using an appropriate riding model (AFIX m3). The final residual values and relevant structure refinement parameters are provided in the Supporting Information. Projection view of the molecules with non-hydrogen atoms represented by 50% probability ellipsoids and showing the atom labeling is presented in Figures 4-6.

Acknowledgment. This work was supported by the University of Missouri-St. Louis Research Award. The support of the NSF (CHE-9318696) and the University of Missouri Research Board are gratefully acknowledged for the purchase of a Varian Unity Plus 300 and Bruker ARX-500 NMR spectrometers. The UM-St. Louis X-ray Crystallography Facility was funded in part by a NSF Instrumentation Grant (CHE-9309690) and the UM-St. Louis Research Award. J.B.-W. is also grateful to Professors Claire Tessier, Joyce Y. Corey, and Peter P. Gaspar for stimulating discussions.

Supporting Information Available: Complete listings of the atomic coordinates, geometrical parameters and anisotropic displacement coefficients for the non-hydrogen atoms, and positional and isotropic displacement coefficients for hydrogen atoms are submitted as Supporting Information for **2-4**. Selected NMR data for **3** are included. This material is available free of charge via the Internet at <http://pubs.acs.org>.

OM000638J

(26) Sheldrick, G. M. Bruker Analytical X-ray; Madison, WI, 1999.

(27) Blessing, R. H. *Acta Crystallogr.* **1995**, *A51*, 33-38.